Multiplexed Relative Quantitation with Isobaric Tagging Mass Spectrometry Reveals Class I Major Histocompatibility Complex Ligand Dynamics in Response to Doxorubicin

J. Patrick Murphy[†], **Qijia Yu**[‡], **Prathyusha Konda**[§], **Joao A. Paulo**[‖], **Mark P. Jedrychowski**[‡,‖],
Daniel J. Kowalewski[⊥,#], **Heiko Schuster**[⊥,#], **Youra Kim**[†], **Derek Clements**[†], **Aditya Jain**[‡],
Stefan Stevanovic[⊥], **Steven P. Gygi**[‖], **Joseph D. Mancias**[*,‡], **Shashi Gujar**[*,†,§,▽]

[†]Department of Pathology, Dalhousie University, Halifax, Nova Scotia B3H 4R2, Canada

[‡]Division of Genomic Stability and DNA Repair, Department of Radiation Oncology, Dana-Farber Cancer Institute, Boston, Massachusetts 02215, United States

[§]Department of Microbiology and Immunology, Dalhousie University, Halifax, Nova Scotia B3H 4R2, Canada

[‖]Department of Cell Biology, Harvard Medical School, Boston, Massachusetts 02115, United States

[⊥]Department of Immunology, Interfaculty Institute for Cell Biology, University of Tubingen, 72076 Tubingen, Germany

[#]Immatics Biotechnologies GmbH, 72076 Tubingen, Germany

[▽]Centre for Innovative and Collaborative Health Systems Research Quality and System Performance, IWK Health Centre, Halifax, Nova Scotia B3K 6R8, Canada

Abstract

MHC-I peptides are intracellular-cleaved peptides, usually 8–11 amino acids in length, which are presented on the cell surface and facilitate CD8^{+} T cell responses. Despite the appreciation of CD8^{+} T-cell antitumor immune responses toward improvement in patient outcomes, the MHC-I peptide ligands that facilitate the response are poorly described. Along these same lines, although many therapies have been recognized for their ability to reinvigorate antitumor CD8^{+} T-cell

[*]**Corresponding Authors**: Tel: (902) 494-1973 (office); (902) 494-2787 (lab). Fax: (902) 494-3292. shashi.gujar@dal.ca.; Tel: (617) 582-9379. joseph_mancias@dfci.harvard.edu.

responses, whether these therapies alter the MHC-I peptide repertoire has not been fully assessed due to the lack of quantitative strategies. We develop a multiplexing platform for screening therapy-induced MHC-I ligands by employing tandem mass tags (TMTs). We applied this approach to measuring responses to doxorubicin, which is known to promote antitumor CD8^{+} T-cell responses during its therapeutic administration in cancer patients. Using both in vitro and in vivo systems, we show successful relative quantitation of MHC-I ligands using TMT-based multiplexing and demonstrate that doxorubicin induces MHC-I peptide ligands that are largely derived from mitotic progression and cell-cycle proteins. This high-throughput MHC-I ligand discovery approach may enable further explorations to understand how small molecules and other therapies alter MHC-I ligand presentation that may be harnessed for CD8^{+} T-cell-based immunotherapies.

Graphical Abstract
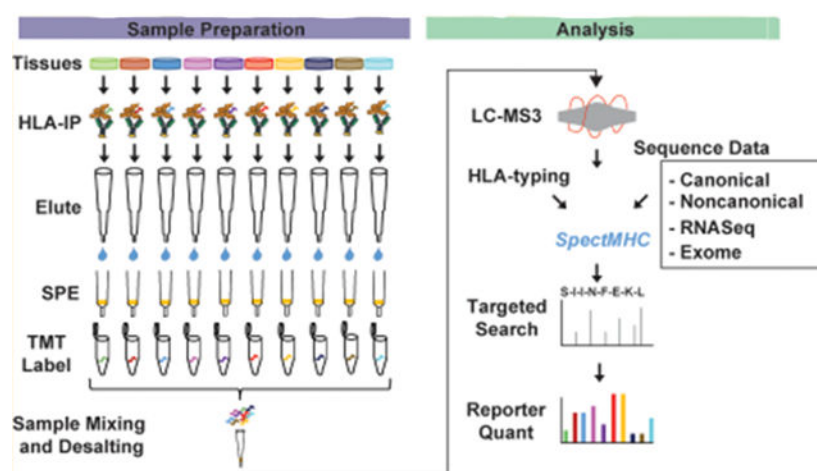
Antigen presentation by Class I Major Histocompatibility Complexes (MHC-I) lies at the crux of CD8^{+} T-cell-mediated immune responses. In the process of antigen presentation, peptide fragments of intracellular-degraded proteins are loaded onto MHC-I molecules, which are subsequently displayed at the cell surface as ligands for recognition by CD8^{+} T cells. Although efforts are being undertaken to predict MHC-I ligands in tumors from genomic data,[1–3] strategies that induce potentially immunogenic MHC-I ligand presentation that may be harnessed to generate antitumor immunity have been largely overlooked. Unlike cancer-specific mutations, differential MHC-I ligand presentation due to, for example, cancer therapies cannot be predicted from genomic data. Furthermore, predicting peptides that form MHC-I ligands from differentially expressed transcripts usually reveals too many candidates to test. Traditional shotgun mass spectrometry immunoprecipitation (MHC-IP-MS) approaches, while able to detect the presence of MHC-I ligand peptides, do not accurately assess changes in their abundance following perturbations. The use of stable isotopic labeling with amino acids (e.g., heavy lysine and arginine) in culture (SILAC) is possible[4] but has limited applicability because (1) many MHC-I peptides do not contain lysine or arginine, (2) patient samples cannot be compared, (3) comparisons are mostly binary, and (4) heavy amino acids are often cost-prohibitive. Alternatively, label-free quantitation (LFQ) approaches can be used but generally suffer from decreased throughput

and missing values across samples.[5] For these reasons, we sought to develop an approach to quantify MHC-I peptides that may be induced by small-molecule therapy.

For multiplexed relative quantitation, isobaric tagging with tandem mass tags (TMTs) allows accurate comparison of 6 to 11 samples in a single experiment.[6] TMT reagents are now widely used in proteomics due to improvements in their accuracy and depth of coverage resulting from new tribrid high-resolution Orbitrap mass spectrometers. In tryptic peptide mixtures, multiplexing with TMT has been hampered by ratio suppression resulting from the coisolation of multiple MS1 spectra. However, methods that utilize an additional (MS3) scan can alleviate ratio suppression. Because purified MHC-I peptide mixtures are usually less complex than tryptic peptide mixtures, MS3-based methods offer comparable (or improved) elimination of ratio suppression. Especially important for low-abundant peptides such as MHC-I ligands, the selection of multiple MS2 peptide ions for the quantitation of TMT reporter ions using synchronous precursor selection (SPS-MS3)[6–9] ensures that sensitivity is not compromised. Finally, using TMT enables the combination of proteome and MHC-I ligandome data to assess the contribution of the source proteome to MHC-I ligand formation. TMT-based relative quantitative comparisons at both the MHC-I ligand and source proteome levels are particularly important because the relationship between source protein turnover and MHC-I peptide abundance is only beginning to be understood.[10,11]

An immediately important application of MHC-I peptide measurement in cancer immunology is to assess the effect of small molecule therapies on the MHC-I ligandome and ultimately gain insight into their effect on antitumor CD8$^+$ T-cell immunity. Anthracyclines, such as doxorubicin, commonly deployed as chemotherapies, are increasingly recognized to enhance antitumor immunity.[12,13] Although induced MHC-I peptides may explain part of the increase in CD8$^+$ T-cell infiltration in tumors treated with doxorubicin and other drugs, the relative determination of peptide induction has not been measured. Here, to gain insight into the effects of small-molecule therapies on the tumor MHC-I ligandome, we developed a TMT-based platform that allows for multiplexed, relative quantitation of the tumor MHC-I ligandome and side-by-side proteome responses. This approach offers a significant improvement in throughput for MHC-I ligandome analysis that can both improve our understanding of the therapy-induced MHC-I ligandomes and provide a means for developing a new class of MHC-I ligandome-based cancer immunotherapies.

■ EXPERIMENTAL SECTION

Doxorubicin Experiments.

HCT116 and EL4 cells were obtained from the American Type Culture Collection and were cultured with DMEM (Gibco) plus 10% FBS (Gibco) and 1% penicillin streptomycin (Gibco) in 37 °C, 5% CO$_2$. C57BL/6 mice were purchased from Charles River (Montreal, QC) and housed in the Dalhousie University Animal Care Facility. For in vitro doxorubicin experiments, HCT116 or EL4 cells were treated with 1 μM doxorubicin. HCT116 cells were treated over a time course of 24 h, harvesting cells at 0, 6, 12, or 24 h. EL4 cells were treated for 48 h. For animal experiments, EL4 cells (5×10^5) were injected subcutaneously into 10 to 16 week old C57BL/6 mice. Following tumor formation (10 days), doxorubicin or PBS

was injected intratumorally (2.5 mg/kg). Tumors and spleens were harvested after 48 h and stored at −80 °C until analysis.

MHC Immunoprecipitation and TMT Labeling.

For cell culture experiments, MHC-I peptides were immunoprecipitated from 1×10^8 cells, as previously outlined.[14] For mouse experiments, two mice in each treatment group were pooled to generate 1 to 2 g of tissue samples (slightly less for spleen samples). MHC-I complexes were purified as previously described[14] using the B22.249 and Y3 antibodies for mouse samples and the W6/32 antibody for human samples. For the parallel analysis of samples, washing and eluting was done on disposable Poly-Prep columns (BioRad) using a vacuum manifold. Peptides were purified using either 3 kDa molecular-weight cutoff (MWCO) filters (Millipore) or solid-phase extraction (SPE) with 60 mg Oasis HLB cartridges (Waters). Peptides were eluted from SPE with 30% acetonitrile (no TFA), then lyophilized. Dried peptides were resuspended in 100 μL of 100 mM Hepes (pH 8.5), 30% acetonitrile, and 10 μL of TMT reagents (Thermo) prealiquoted at a final concentration of 20 μg/mL in anhydrous acetonitrile, mixed and desalted using Stage tips.[15]

LC-SPS-MS3 Analysis for MHC-I Peptides and Proteins.

Dried TMT-labeled peptides were resuspended in 6 μL of 1% formic acid; then, 2 μL was loaded onto a column and analyzed using an Orbitrap Fusion Lumos mass spectrometer (Thermo Fisher Scientific, San Jose, CA) coupled to a Proxeon EASY-nLC 1200 liquid chromatography (LC) pump (Thermo Fisher Scientific). Peptides were separated on a 100 μm inner diameter microcapillary column packed with 35 cm of Accucore C18 resin (2.6 μM, 150 Å, Thermo Fisher). Peptides were separated at a flow rate of ~500 nL/min using a gradient of 3–22% acetonitrile (0.125% formic acid) over 120 min and analyzed by SPS-MS3. MS1 scans were acquired over an m/z range of 300–800, 60K resolution, AGC target of 5e5, and maximum injection time of 250 ms. MS2 scans were acquired on MS1 ions of charge state 2 to 3 using an isolation window of 0.7 Th, collision-induced dissociation (CID) activation with a collision energy of 35%, rapid scan rate, AGC target of 5000, and maximum injection time of 150 ms. MS3 scans were acquired using SPS of 15 isolation notches, m/z range of 100–1000, 15K resolution, AGC target of 5e5, higher-energy collisional dissociation (HCD) activation at 55%, and maximum injection time of 300 ms. Each sample was injected twice with dynamic exclusion of 10 or 30 s (after 1 MS2, with an 8 ppm tolerance window). The global cycle time for the method was set at 3 s. SpectMHC-enabled database searching was performed as previously described.[14] The summed reporter ion S/N for all spectral matches (PSMs) for each peptide was used for relative quantitation and normalized within each channel using the summed S/N for all compared peptides. MHC-I purity was assessed by "no enzyme" searches, as previously described.[14] For multiplexed proteomics, cells were lysed, digested, and TMT-labeled, SPS-MS3 was performed on 12 high-pH reversed-phase fractions collected on the Orbitrap Fusion Lumos, and proteins were identified and quantified as previously described.[16] Statistical analyses of the quantitative proteome and peptidome data were performed in R.

■ RESULTS AND DISCUSSION

Development of a Platform for Multiplexed MHC-I Peptide Analysis To Assess the Effects of Therapy.

To measure MHC-I peptide differences, we developed a platform using TMT-based multiplexing and SPS-MS3 analysis. The method utilizes SpectMHC-enabled targeted searches,[14] ensuring the relative quantification of several thousand MHC-I peptides from 1 to 2 g of tissue, rivalling nonquantitative shotgun analyses.[17] The procedure begins by immunoprecipitating MHC-I or Human Leukocyte Antigen (HLA) complexes from ~1 to 2 g of tissue or cell pellet using anti-MHC-I (mouse) or pan anti-HLA (human) antibodies. Peptides are then released from antibodies by acidification, purified using MWCO or SPE, TMT-labeled, analyzed by SPS-MS3, and identified by a targeted database search (Figure 1). Proteome databases can be derived from mouse/human reference assemblies, RNASeq data, whole exome data, or noncanonically translated sequences, providing a means to quantify changes in self or potential neoantigens. Data sets contain relative quantitation for 2000–5000 MHC peptides across 6–11 conditions, representing the first report of global, multiplexed MHC-I peptide comparisons by isobaric tagging. Although several other studies have used SILAC and pulse-chase approaches to determine how protein turnover and abundance affect the MHC-I ligandome,[10,18,19] this problem has not been assessed by matching relative peptide and protein quantitation, as we have done here.

We postulated that purification and TMT labeling steps could alter the properties of peptides identified as MHC-I peptides. As such, we assessed whether purification by MWCO or SPE, as well as TMT labeling, affects the number of identified peptides and their amino acid composition. A preliminary comparison of MWCO- and SPE-based methods in a non-TMT-labeled LC-MS2 experiment showed high purity (>90% of peptides had NetMHC ranks <2%) and increased peptide identifications by targeted searching, resulting in 2768 and 1704 unique MHC-I peptide identifications from human colorectal (HCT116) and breast (MDA MB 468) cancer cell lines, respectively (Figure S1,B). Only minor differences in the number of peptide identifications were observed between MWCO and SPE purifications (Figure S1A,B). Although peptide identities between MWCO- and SPE-purified samples showed incomplete overlap (Figure S1C,D), we found few differences in the amino acid composition of MWCO-unique and SPE-unique peptides (Figure S1E), suggesting that there appears to be negligible amino acid frequency bias for either of the purification methods. The exceptions were that MWCO-unique peptides were generally composed of a greater proportion of nonpolar (and fewer polar) amino acids, whereas SPE-unique peptides were composed of more charged amino acids (Figure S1E).

We next compared MWCO and SPE purification using nonisotopic TMT reagent (TMT0[126]), using SPS-MS3 for analysis. A single HLA-IP from MDA MB 468 cells was equally apportioned to samples for MWCO, SPE (both analyzed by SPS-MS3), or unlabeled MWCO-purified peptides for analysis by MS2 (Figure 2A). Using a targeted search, we identified 4537 unique HLA peptides across the three samples, a slight improvement over a reference search (Figure S2A). For the TMT0[126]-labeled samples, we observed 1.5 times more peptide identifications from the SPE-purified than MWCO-purified sample (Figure

2B). Fewer peptide identifications by MS3 than MS2 were due to slower cycle times (Figure S2B). Although incomplete overlap was observed (Figure 2C), the amino acid composition of peptides unique to either TMT0[126]-labeled or unlabeled samples was similar (Figure 2D), suggesting no biases due to TMT labeling. Within the TMT0[126]-labeled samples, incomplete overlap was observed between the SPE-and MWCO-purified samples (Figure 2E), and we observed a higher average TMT0[126] S/N for SPE-than MWCO-purified samples (Figure 2F). Also, more peptides had TMT0[126] S/N greater than 1000 in the SPE-purified samples (Figure 2G), suggesting that SPE purification is more robust than MWCO for TMT labeling. As such, we prefer the use of SPE purification for the remainder of our analyses.

In proteomics, tryptic peptides with lysine residues in the C-termini generate y ion MS2 fragments that contain TMT reporter ions when fragmented by MS3. In MHC-I peptides, y ions of peptide MS2 fragments contain a TMT tag only if a lysine is present, which may seldom occur at the C-terminus. In these cases, only b ions isolated for MS3 contain reporter ions, potentially limiting the sensitivity of SPS-MS3. We indeed observed slightly lower average TMT0[126] S/N for TMT-labeled peptides without lysine residues anywhere in the sequence in both MWCO- and SPE-purified samples (Figure 2H). In agreement with the increased S/N in the SPE sample, 51 and 43% of the peptides quantified by SPE and MWCO, respectively, contain lysines (Figure 2I). However, the presence of lysine had little effect on the number of peptides with acceptable S/N ranges (>100) (Figure 2I). These data confirm that SPS-MS3 analysis of TMT-labeled MHC-I peptides is a feasible quantitative approach.

MHC-I Peptides from Chromatin-Related Proteins Are Induced by Doxorubicin.

The recognized induction of immunogenic cell death (ICD) by anthracyclines[12,13] prompted us to measure changes in the MHC-I peptidome following doxorubicin treatment. In duplicate, HCT116 cells were treated with doxorubicin (1 μM) over 24 h with four time points from which 8-plex MHC-I peptidomic and source proteomics was performed with SPS-MS3 (Figure 3A). A total of 3349 unique MHC-I peptides were identified using a targeted search, of which 3202 were compared across all eight samples, a 1.4-fold increase over a reference database search (Figure S3). Most of the MHC-I peptide differences began to appear between 12 and 24 h (Figure 3B), suggesting that alterations in antigen presentation following stress such as doxorubicin treatment are not immediate. We observed the significant induction of 239 peptides ($\log_2$(fold change) > 2 and F-test p value <0.05) at 24 h doxorubicin treatment (Figure 3B). Interestingly, the source proteins for these 239 induced peptides are significantly enriched in GO terms (biological process) for nucleic acid metabolism and the nucleus (cellular compartment) (Figure 3C). Source proteins from this group include a range of proteins related to chromatin remodelling and chromosome segregation (Figure 3D). The enrichment of MHC-I peptides from source transcripts/ proteins associated with the cell cycle is remarkable given the known cell-cycle arrest induced by doxorubicin.

We successfully matched 2617 (82%) quantified peptide sequences to 6586 proteins in the proteome data set, creating 2766 relative quantitative peptide/source protein combinations. Interestingly, we observed almost no correlation between the $\log_2$(fold changes) of the HLA

peptide and source protein at 24 h (Figure 3E). For example, many of the highly induced chromatin-related proteins (MEX3D, RFC4, UTP4, and FZR1) showed very stable abundance in the quantitative proteome data set (Figure 3F). This was also mostly true for the highly down-regulated proteins, exemplified by COPG1 and TMED10 (Figure 3G). We did, however, observe the induction of peptides for MDM2 and KLHL21 (both of which play a role in DNA repair and chromatin interaction) at both the source protein and MHC-I peptide levels (Figure 3H). MDM2 is an E3 ubiquitin ligase for p53,[20] from which, unfortunately, no MHC-I peptides were identified in the mouse experiment. HCT116 cells, used in our analysis, are wild-type for p53, and it has been previously shown that anthracyclines (including doxorubicin) increase the levels of p53,[21] consistent with our observed increases in MDM2 and associated MHC-I peptides derived thereof.

Relative Quantitation of MHC Peptides in an EL4 Mouse Tumor Model of Doxorubicin Treatment.

Whereas we observed clear differences due to doxorubicin in cell lines, it is important to understand systemic effects. We thus employed our multiplexing methodology to measure MHC-I peptides and their source proteins in C57BL/6 mice bearing syngeneic EL4 lymphoma tumors. MHC-I peptides were immunoprecipitated from (1) in vitro cultured EL4 cells, (2) subcutaneous EL4 tumors, and (3) spleens from EL4 tumorbearing mice, each treated with vehicle (PBS) or 2.5 mg/kg doxorubicin (Figure 4A). MHC-I IPs were performed with allele-specific antibodies to both the H-2D^b (B22.249 hybridoma clone) and the H-2K^b (Y3 hybridoma clone) mouse MHC-I alleles and analyzed by two separate TMT 10-plex experiments. With SpectMHC, we identified 3600 unique MHC-I peptides (NetMHC Rank <2%), 1997 H-2D^b and 1603 H-2K^b, a two-fold increase compared with a reference database search (Figure S4A). Of these, relative quantitation was successful (summed S/N > 100) for 3460 MHC-I peptides (96%) across the samples (Figure S4A). We observed 33 and 27 MHC peptides significantly ($p < 0.05$) increased or decreased, respectively, in the EL4 tumor (in vivo) in response to treatment with doxorubicin (Figure 4B). Consistent with our in vitro results, we observed significant induction of several MHC-I peptides from source proteins with functions related to chromatin and mitotic transition. (Figure 4C). For example, an MHC-I peptide derived from the nucleosome-related protein NPM1 was significantly induced (in the in vivo tumor only) with doxorubicin treatment (Figure S4B). Interestingly, in the HCT116 in vitro experiment, we also observed the induction of separate MHC-I peptides from NPM1. Furthermore, peptides from the putative cytokinesis and spermatogenesis protein SEPT4 and SPATA20 were also induced by doxorubicin in the EL4 tumors (Figure S4B). We next determined whether these effects were shared with protein responses. We successfully matched 1105 H-2D^b (64%) and 915 (65%) H-2K^b MHC-I peptides to the proteomics data set, creating 2534 peptide/source protein pairs (Figure 4E). Like our in vitro experiment, there was almost no correlation between the MHC-I peptide log$_2$(fold changes) and the source protein log$_2$(fold changes) at 24 h for both the spleen and tumor data (Figure 4F).

Principal component analysis (PCA) of the MHC-I data set revealed tight clustering of the replicates (in vitro only), demonstrating not only the robustness of the data but also that samples from the tissue of origin projected separately. Clear separation between in vivo and

in vitro tissues superseded that of doxorubicin (Figure 5A). For example, 260 MHC-I peptides had >60% of their relative TMT intensity (based on summed S/N) from the spleen samples (Figure 5B). Likewise, 126 and 13 MHC-I peptides had >60% of their relative intensity from the in vitro and in vivo EL4 samples, respectively (Figure 5B). As such, the tissue of origin has a strong effect on the MHC-I peptide composition, as exemplified by several MHC-I peptides derived from source proteins of various functions (Figure S4C). The source proteomics data set (6585 proteins) showed distinct protein abundance patterns across the samples (Figure S5A), including the induction of several proteins in the tumor such as PLIN1 and PLIN4 (Figure S5B). Like the MHC-I peptide data, replicate samples in the proteome-level PCA analysis clustered together, and tissues of origin projected separately (Figure S5C,D). We again observed poor MHC-I peptide and source protein correlations (Figure S5E), except for several tissue-specific MHC-I peptides such as CCL8 and MYLK (Figure S5F). The limited number of source protein and MHC-I peptide correlations highlight complex differences in protein homeostasis and antigen processing.[22]

Because poor MHC-I peptide and source protein correlations could result from differential protein cleavage, we examined upstream and downstream flanking sequences (+ or − 5 amino acid residues). The 33 doxorubicin-induced MHC-I peptides in the in vivo tumor had very different flanking amino acid frequencies compared with those with no change (or decrease) across the samples (Figure S6A). More numerous differences across tissues allowed us to examine flanking sequences in larger lists of peptides by comparing the source proteins of highly tissue-specific MHC-I peptides. Again, we observed strikingly different patterns in amino acid frequencies in the flanking sequences of MHC-I peptides that were tissue-specific than in those that were equal across all samples (Figure 5C). More specifically, arginine residues were more frequent +5 from the MHC-I peptide in the spleen-specific residues, whereas leucine was more frequent at the same position in the in vitro tumor-specific residues (Figure 5D). We also find that induced MHC-I peptides were, on average, slightly closer to the C-terminus (Figure S6B). Furthermore, of the tissue-specific MHC-I peptides, the EL4 tumor peptides (both in vitro and in vivo) were also closer to the C-terminus (Figure S6C). These data suggest that flanking sequences play a large role in MHC-I peptide abundance.

■ CONCLUSIONS

Altogether, our data demonstrate the utility of isobaric tagging of MHC-I peptides with TMT to measure the induction of new MHC-I peptides by small-molecule therapy that may elicit a CD8^{+} T-cell-mediated immune response. The mass spectrometry proteomics data have been deposited to the ProteomeXchange Consortium via the PRIDE partner repository[23] with the data set identifiers PXD011464 (HCT116 cell time-course doxorubicin) and PXD011444 (EL4 tumors with doxorubicin). Currently, LFQ is the most widely used approach to estimate MHC-I ligand differences between samples. Interestingly, our recent exhaustive comparison of LFQ- and TMT-based approaches for tryptic mixtures showed a higher number of missing values for LFQ and better statistics for low-abundance peptides.[24] Here we also observed few missing values across samples for both in vitro and in vivo experiments and tight clustering of replicates by PCA. These data highlight the precision of TMT measurements and the ability to obtain accurate relative quantitation of

low-abundance peptides (here MHC-I peptides), which is often difficult to achieve with LFQ.

Additional data sets will be necessary to understand whether the induction of mitotic transition proteins is conserved across many cell lines and tumors and, crucially, whether these therapy-induced peptides elicit antitumor CD8^{+} T-cell immune responses. Our platform may also be employed to better determine the factors that govern antigen presentation from source proteins. For example, the multiplexing capabilities of TMT combined with heavy amino acids could reveal the stoichiometric contributions of protein turnover, translation, altered proteasomal cleavage, and peptide trimming to the abundance of an MHC-I peptide. Furthermore, although we here have explored therapeutically derived changes, many other scenarios may alter the MHC-I ligandome such as infection or cell stress. Finally, emerging labeling strategies such as combinatorial isobaric mass tags (CMTs) will facilitate the comparison of 28 samples simultaneously,[25] paving the way for high-throughput screens that elicit changes in MHC-I ligandomes.

Supplementary Material

Refer to Web version on PubMed Central for supplementary material.

■ ACKNOWLEDGMENTS

■ REFERENCES

(1). Matsushita H; Vesely MD; Koboldt DC; Rickert CG; Uppaluri R; Magrini VJ; Arthur CD; White JM; Chen Y-S; Shea LK; et al. Nature 2012, 482 (7385), 400–404. [PubMed: 22318521]

(2). Castle JC; Kreiter S; Diekmann J; Lower M; van de Roemer N; de Graaf J; Selmi A; Diken M; Boegel S; Paret C; et al. Cancer Res. 2012, 72 (5), 1081–1091. [PubMed: 22237626]

(3). Yadav M; Jhunjhunwala S; Phung QT; Lupardus P; Tanguay J; Bumbaca S; Franci C; Cheung TK; Fritsche J; Weinschenk T; et al. Nature 2014, 515 (7528), 572–576. [PubMed: 25428506]

(4). Lemmel C; Weik S; Eberle U; Dengjel J; Kratt T; Becker H-D; Rammensee H-G; Stevanović S Nat. Biotechnol 2004, 22 (4), 450–454. [PubMed: 15004565]

(5). Cox J; Hein MY; Luber CA; Paron I; Nagaraj N; Mann M Mol. Cell. Proteomics 2014, 13 (9), 2513–2526. [PubMed: 24942700]

(6). McAlister GC; Huttlin EL; Haas W; Ting L; Jedrychowski MP; Rogers JC; Kuhn K; Pike I; Grothe RA; Blethrow JD; et al. Anal. Chem 2012, 84 (17), 7469–7478. [PubMed: 22880955]

(7). Ting L; Rad R; Gygi SP; Haas W Nat. Methods 2011, 8 (11), 937–940. [PubMed: 21963607]

(8). McAlister GC; Nusinow DP; Jedrychowski MP; Wühr M; Huttlin EL; Erickson BK; Rad R; Haas W; Gygi SP Anal. Chem 2014, 86, 7150–7158. [PubMed: 24927332]

(9). Murphy JP; Stepanova E; Everley RA; Paulo JA; Gygi SP Mol. Cell. Proteomics 2015, 14 (9), 2454–2465. [PubMed: 26077900]

(10). Bassani-Sternberg M; Pletscher-Frankild S; Jensen LJ; Mann M Mol. Cell. Proteomics 2015, 14 (3), 658–673. [PubMed: 25576301]

(11). Bourdetsky D; Schmelzer CEH; Admon A Proc. Natl. Acad. Sci. U. S. A 2014, 111, E1591–E1599. [PubMed: 24715725]

(12). Apetoh L; Mignot G; Panaretakis T; Kroemer G; Zitvogel L Trends Mol. Med 2008, 14 (4), 141–151. [PubMed: 18353726]

(13). Casares N; Pequignot MO; Tesniere A; Ghiringhelli F; Roux S; Chaput N; Schmitt E; Hamai A; Hervas-Stubbs S; Obeid M; et al. J. Exp. Med 2005, 202 (12), 1691–1701. [PubMed: 16365148]

(14). Murphy JP; Konda P; Kowalewski DJ; Schuster H; Clements D; Kim Y; Cohen AM; Sharif T; Nielsen M; Stevanovi S; et al. J. Proteome Res 2017, 16, 1806–1816. [PubMed: 28244318]

(15). Rappsilber J; Ishihama Y; Mann M Anal. Chem 2003, 75, 663–670. [PubMed: 12585499]

(16). Clements DR; Murphy JP; Sterea A; Kennedy BE; Kim Y; Helson E; Almasi S; Holay N; Konda P; Paulo JA J. Proteome Res 2017, 16, 3391. [PubMed: 28768414]

(17). Bassani-Sternberg M; Braunlein E; Klar R; Engleitner T; Sinitcyn P; Audehm S; Straub M; Weber J; Slotta-Huspenina J; Specht K; et al. Nat. Commun 2016, 7, 13404–13420. [PubMed: 27869121]

(18). Milner E; Gutter-Kapon L; Bassani-Strenberg M; Barnea E; Beer I; Admon A Mol. Cell. Proteomics 2013, 12 (7), 1853–1864. [PubMed: 23538226]

(19). Milner E; Barnea E; Beer I; Admon A Mol. Cell. Proteomics 2006, 5 (2), 357–365. [PubMed: 16272561]

(20). Honda R; Tanaka H; Yasuda H FEBS Lett. 1997, 420 (1), 25–27. [PubMed: 9450543]

(21). Bug M; Dobbelstein M Oncogene 2011, 30 (33), 3612–3624. [PubMed: 21441950]

(22). Liepe J; Marino F; Sidney J; Jeko A; Bunting DE; Sette A; Kloetzel PM; Stumpf MPH; Heck AJR; Mishto M Science 2016, 354 (6310), 354–358. [PubMed: 27846572]

(23). Vizcaino JA; Csordas A; del-Toro N; Dianes JA; Griss J; Lavidas I; Mayer G; Perez-Riverol Y; Reisinger F; Ternent T; et al. Nucleic Acids Res. 2016, 44 (D1), D447–D456. [PubMed: 26527722]

(24). O'Connell JD; Paulo JA; O'Brien JJ; Gygi SP J. Proteome Res 2018, 17, 1934–1942. [PubMed: 29635916]

(25). Braun CR; Bird GH; Wuhr M; Erickson BK; Rad R; Walensky LD; Gygi SP; Haas W Anal. Chem 2015, 87, 9855–9863. [PubMed: 26308379]
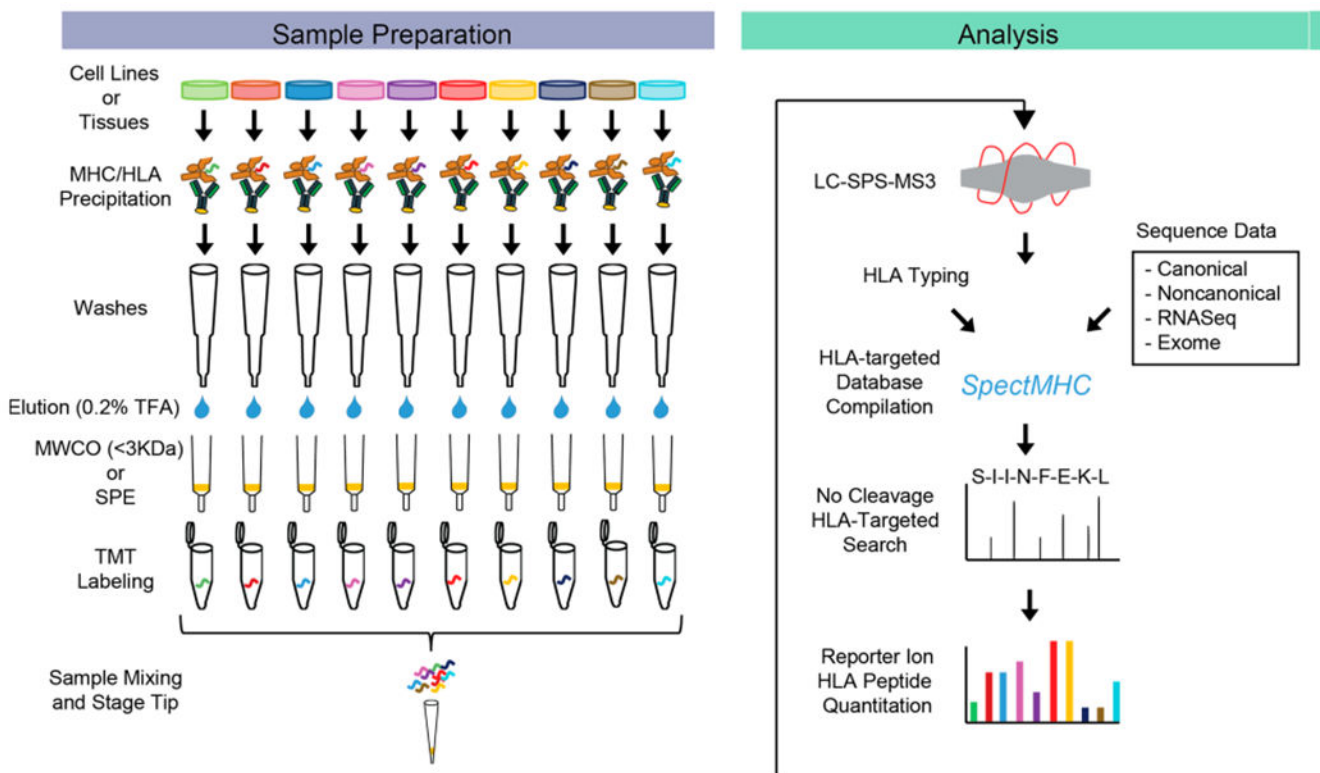
Figure 1.
Platform for relative quantitative and multiplexed MHC-I peptidome analysis with TMT. Experiments begin with 6 to 11 samples (1 to 2 g of tissue or cell pellet per sample), followed by lysis, immunoprecipitation with an MHC/HLA-specific antibody, washing, and acid elution. Optionally, prior to lysis, a small portion of the sample can be saved for matched proteomic or proteogenomic analysis. Peptides are purified directly using MWCO or SPE and desalted using a Stage tip. Accurate relative quantitation between samples is achieved by SPS-MS3 data acquisition, and maximal HLA peptide identification is achieved with a targeted search strategy (enabled by SpectMHC) based on tissue HLA types. Optionally, exome or RNASeq data can be integrated into the targeted database. Finally, summed reporter ion intensities (S/N) represent individual HLA peptide relative quantitation across samples.
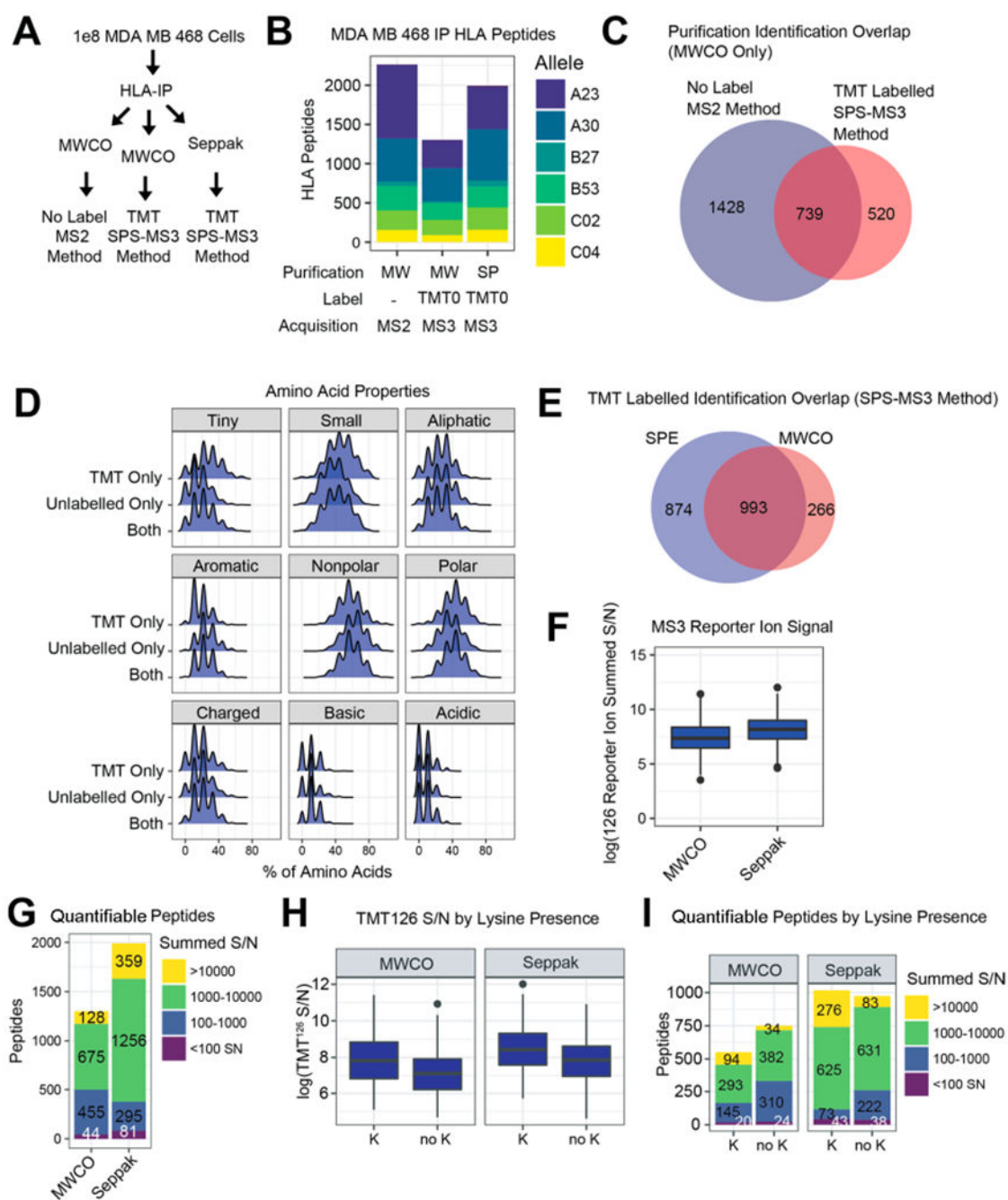
Figure 2.

Effects of purification and TMT labeling on MHC-I peptidome composition. (A) Schematic to compare MWCO and SPE MHC-I peptide purification for TMT labeling in MDA MB 468 cells using TMT0. (B) Number of identified TMT0-labeled peptides by MWCO and SPE methods (both analyzed by SPS-MS3) compared with a standard MWCO and LC-MS2 method. (C) Overlap between TMT0-labeled and unlabeled HLA peptides (MWCO only). (D) Amino acid properties for MHC-I peptides found in the groups from panel C. (E) Overlap between MWCO- and SPE-purified TMT0-labeled HLA. (F) Comparison of logged

signal-to-noise values of the TMT0 126 reporter ion between MWCO- and SPE-purified TMT0-labeled HLA peptides. (G) Quantifiable peptides (S/N > 100) in the TM0-labeled samples purified by either MWCO or SPE. (H) Mean logged S/N among peptides with or without the presence of lysine (K) in the sequence. (I) Quantifiable peptides in different S/N ranges among peptides with or without the presence of K in the sequence.
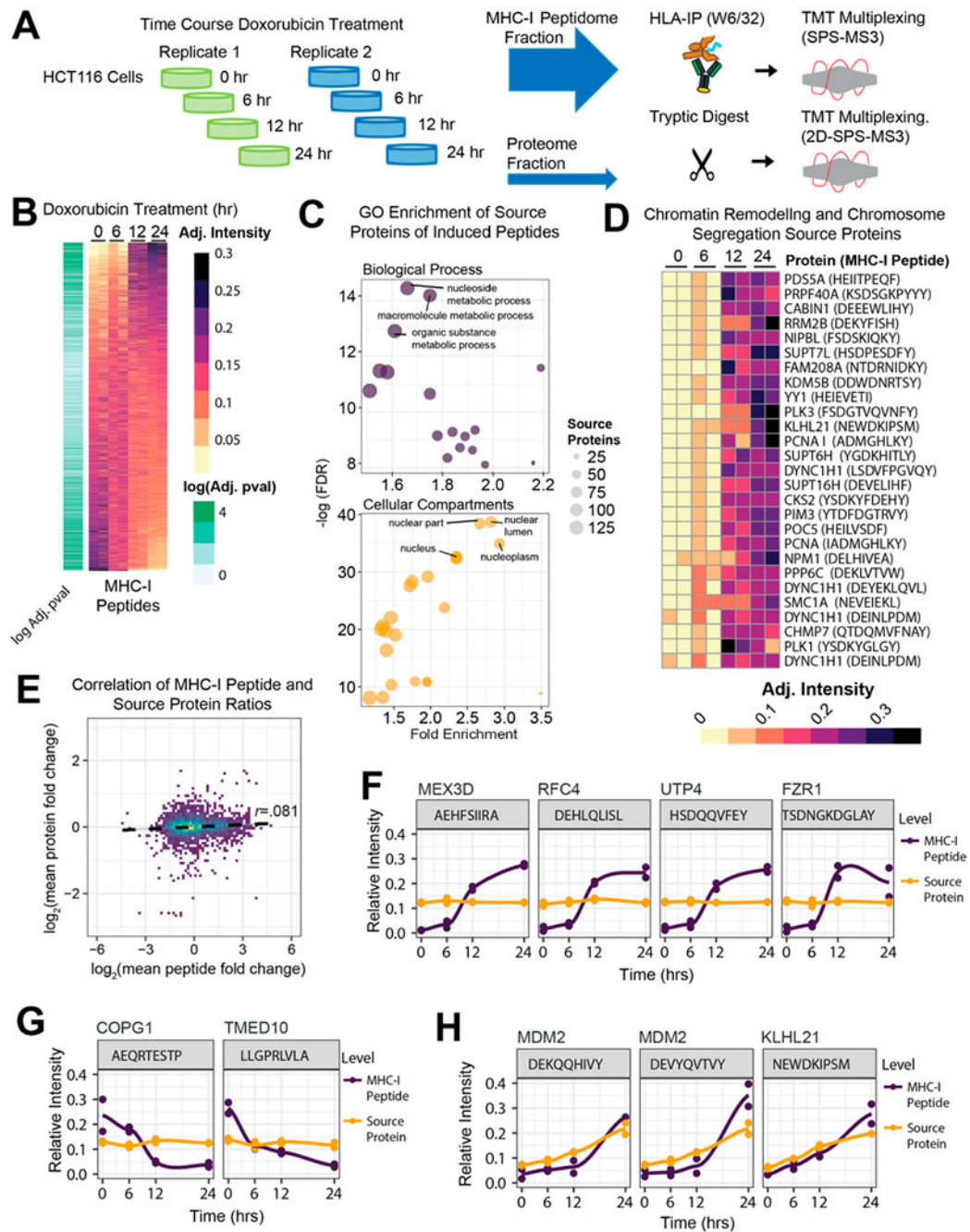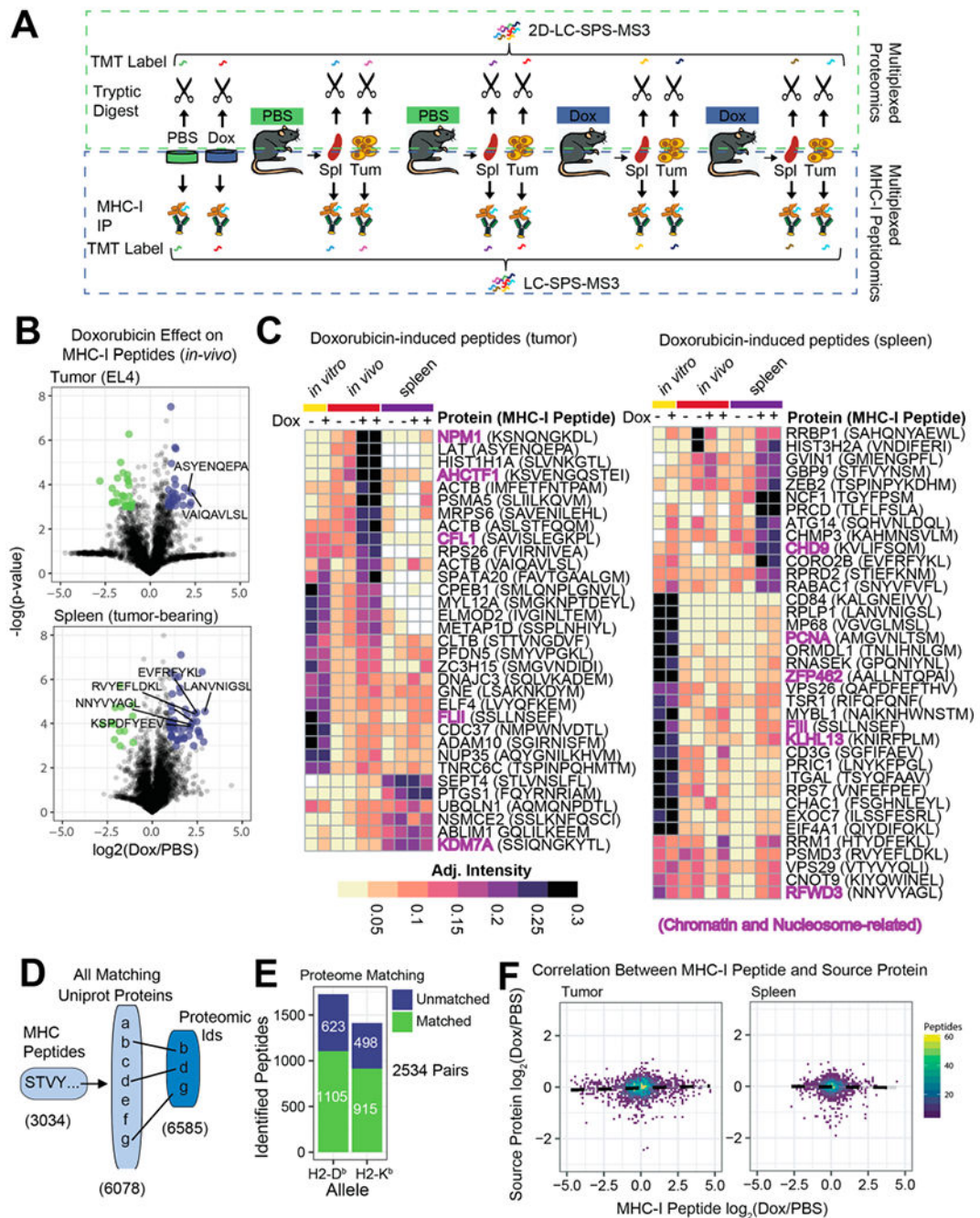
Figure 3.
Dynamic, temporal induction of MHC-I peptides from chromatin and nucleosomal source proteins during time-course doxorubicin treatment of colon cancer cells. (A) Experimental schematic. HCT116 cells were treated over 24 h with 1 μM doxorubicin in duplicate. Cells were divided into MHC-I peptidome and proteome portions (90 and 10%, respectively) and subjected to MHC-I IP or tryptic digest, followed by multiplexed analyses with SPS-MS3. (B) Heatmap of global MHC-I peptide relative abundance over time. (C) Enriched GO terms (both Biological Process and Cellular Compartment) highlighting nuclear associations

among doxorubicin-induced proteins. (D) Heatmap showing examples of highly induced MHC-I peptides from chromatin and chromosome segregation proteins. (E) Overall correlation between the mean relative peptide and matching mean source protein level changes after 24 h of doxorubicin treatment. (F) Examples of doxorubicin-induced MHC-I peptides from several nuclear-associated proteins (with no measurable change in the source proteins). (G) Examples of doxorubicin-repressed MHC-I peptides (associated with vesicle trafficking). (H) MHC-I peptides induced at the peptide and source levels, including two MHC-I peptides from MDM2 and one from KLHL21, both cell-cycle-related ubiquitin E3 ubiquitin ligases. Log Adj. pval = Benjamini–Hochberg-corrected F-test p value.

Figure 4.
MHC-I peptide multiplexing in a mouse tumor model of doxorubicin treatment. (A) Experimental setup. Tumors (EL4 lymphoma) and spleens ($n = 2$) from mice treated or untreated with 2.5 mg/kg doxorubicin or vehicle (PBS) were harvested and subjected to multiplexed MHC-I peptidome or proteome analysis. Cultured EL4 cells (doxorubicin- or PBS-treated, $n = 1$) were also included as a comparison. (B) Volcano plot of doxorubicin effects on the MHC-I peptides in the EL4 tumors and spleens from the same mice. (C) Heatmaps of doxorubicin-induced MHC-I peptides from both the tumor (left) and the spleen
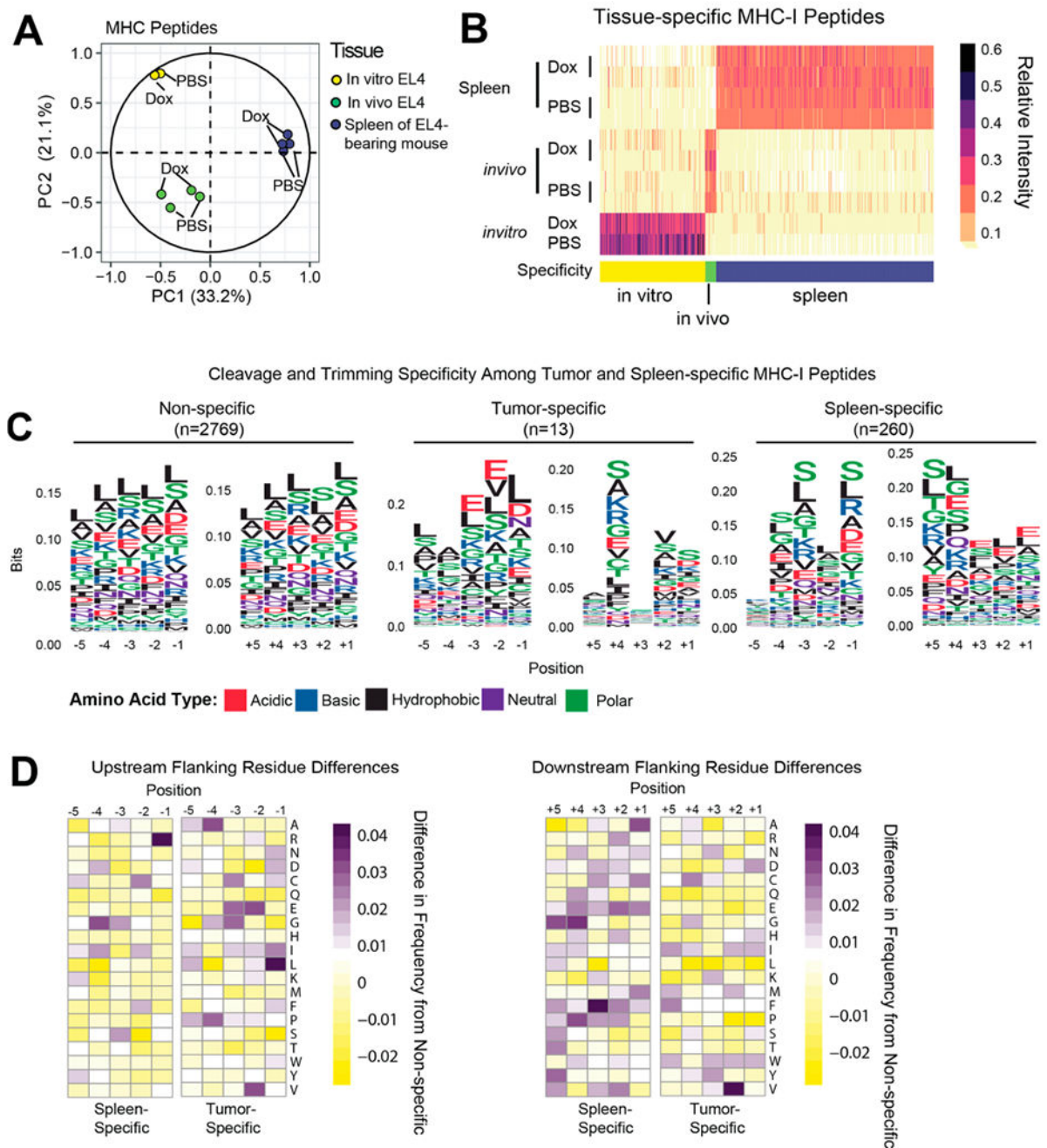
(right) as they appear across all 10 samples. (D) Strategy for matching MHC-I peptides to potential source proteins. (E) Number of MHC-I peptides (with H-2 K^b or H-2 D^b specificity) matching the multiplexed proteome data set. (F) Correlation of doxorubicin-induced changes in both the tumor (left) and spleen (right) at the MHC-I peptide and source protein levels.

Figure 5.

Tissue specificity in relative quantitative MHC-I peptidome data from the EL4 mouse tumor model with doxorubicin. (A) Principal component analysis (PCA) of multiplexed MHC-I peptide data in the EL4 tumor model experiment. (B) Heatmap of MHC-I peptides (3034 unique peptides) specific to spleen, tumor, or in vitro tumors, independent of doxorubicin treatment. (C) Sequence logos demonstrating upstream and downstream proteasomal cleavage and trimming specificity of tumor- and spleen-specific MHC-I peptides (compared

with nonspecific peptides). (D) Differential frequency of amino acids in the upstream and downstream sequences of spleen- and tumor-specific MHC-I peptides.